Biomedicine & Pharmacotherapy 68 (2014) 1007–1014

Available online at
ScienceDirect
www.sciencedirect.com

Elsevier Masson France
EM|consulte
www.em-consulte.com/en

Original article

Antroquinonol blocks Ras and Rho signaling via the inhibition of protein isoprenyltransferase activity in cancer cells

Ching-Liang Ho [a], Jui-Ling Wang [b], Cheng-Chung Lee [c], Hsiu-Yi Cheng [d], Wu-Che Wen [d], Howard Hao-Yu Cheng [d], Miles Chih-Ming Chen [d,*]

[a] Division of Hematology/Oncology, Department of Internal Medicine, Tri-Service General Hospital, Neihu, 114, Taipei, Taiwan, ROC
[b] Agriculture Biotechnology Research Center, Academia Sinica, Nankang, 115 Taipei, Taiwan, ROC
[c] National Core Facilities for Protein Structural Analysis, Nankang, 115 Taipei, Taiwan, ROC
[d] Division of Biological Chemistry, Golden Biotechnology Corp., Danshui Dist., 251 New Taipei City, Taiwan, ROC

ARTICLE INFO

Article history:
Received 6 August 2014
Accepted 14 September 2014

Keywords:
Antroquinonol
Ras
Farnesyltransferase
Prenylation
Autophagy

ABSTRACT

Antroquinonol is the smallest anticancer molecule isolated from *Antrodia camphorata* thus far. The ubiquinone-like structure of Antroquinonol exhibits a broad spectrum of activity against malignancies in vivo and in vitro. However, the mechanism of action of Antroquinonol remains unclear. Here, we provide evidence that Antroquinonol plays a role in the inhibition of Ras and Ras-related small GTP-binding protein functions through the inhibition of protein isoprenyl transferase activity in cancer cells. Using cell line-based assays, we found that the inactive forms of Ras and Rho proteins were significantly elevated after treatment with Antroquinonol. We also demonstrated that Antroquinonol binds directly to farnesyltransferase and geranylgeranyltransferase-I, which are key enzymes involved in activation of Ras-related proteins, and inhibits enzymes activities in vitro. Furthermore, a molecular docking analysis illustrated that the isoprenoid moiety of Antroquinonol binds along the hydrophobic cavity of farnesyltransferase similar to its natural substrate, farnesyl pyrophosphate. In contrast, the ring structure of Antroquinonol lies adjacent to the Ras-CAAX motif-binding site on farnesyltransferase. The molecular docking study also showed a reasonable correlation with the IC_{50} values of Antroquinonol analogues. We also found that the levels of LC3B-II and the autophagosome-associated LC3 form were also significantly increased in H838 after Antroquinonol administration. In conclusion, Antroquinonol inhibited Ras and Ras-related GTP-binding protein activation through inhibition of protein isoprenyl transferase activity, leading to activation of autophagy and associated mode of cell death in cancer cells.

1. Introduction

Natural products have traditionally been an important source of organic chemicals and pharmaceuticals. More than 20 new drugs derived from natural sources have been launched on the market during the past 10 years [1]. We adopted an anticancer drug screen model to test the anticancer effects of crude extracts of Chinese herbs, plants, and fungi collected in Taiwan. Anticancer activities were identified in *Antrodia camphorata*, a species of fungus endemic to Taiwan [2]. Antroquinonol is a new chemical entity isolated from the mycelium of *A. camphorata* that showed interesting anticancer and anti-inflammatory activities [3–5]. Previous studies have indicated that signaling molecules, such as PI3K, AMPK, and mTOR, participated in Antroquinonol-induced cancer cell death, whereas Nrf2 and NF-kB were involved in the anti-inflammatory effects of Antroquinonol [3,4,6]. However, the precise mechanism of action remains unknown.

Yu et al. reported that Antroquinonol caused a mobility shift of the Ras protein on immunoblots [7], suggesting that Antroquinonol-mediated Ras expression and activation in cancer cells. Ras proteins have been considered drug targets due to gain-of-function mutations in approximately 30% of all human cancers [8]. Ras undergoes posttranslational processing to become a biologically active protein that is embedded in the plasma membrane. Prenylation is mediated by isoprenyltransferase such as farnesyltransferase (FTase) and geranylgeranyltransferase-1 (GGTase-1),

* Corresponding author. Golden Biotechnology Corp, 10F, No. 9, Ln. 3, Jhong-Jheng E. Rd., Danshui Dist., 251 New Taipei City, Taiwan, ROC.
Tel.: +886 2 2626 1810x225; fax: +886 2 2626 1812.
E-mail addresses: miles@goldenbiotech.com.tw, milesjlw@yahoo.com.tw (M.-M. Chen).

http://dx.doi.org/10.1016/j.biopha.2014.09.008
0753-3322/

and is the first committed step for Ras processing [9]. FTase, for example, covalently transfers a 15-carbon isoprenyl group from farnesyl pyrophosphate (FPP) to the cysteine residue of the conserved CAAX motif in the C-terminus of Ras [10].

FTase inhibitors (FTIs) represent a new class of anticancer agents that inhibit Ras prenylation. Several FTIs that mimic the structures of the FTase substrates, farnesyl pyrophosphate (FPP) and CAAX tetrapeptides, have been developed and are currently being evaluated in clinical trials [11]. However, the results are not entirely promising. Two main questions driving preclinical and clinical studies of FTIs are whether Ras can be alternatively prenylated by GGTase-1 and whether inhibition of FTase can affect proteins other than Ras. Evidence indicates that most FTIs specifically inhibit FTase but not GGTase-1 in vitro and in vivo [12–14]. As a result, alternative prenylation of K-Ras and N-Ras by the attachment of a 20-carbon geranylgeranyl chain by GGTase-I has been reported in FTI-treated cells [15,16]. Furthermore, cells with wild-type or mutant Ras were sensitive to FTIs in vitro and in vivo [13,17]. Collectively, these observations indicate that prenylated proteins other than Ras might also contribute to the anticancer activities of FTIs. Thus, further investigation of an active prenyltransferase inhibitor that blocks the growth of Ras-dependent and Ras-independent cancer cells is warranted.

In this study, we used molecular docking techniques combined with biochemistry, molecular biology, and medicinal chemistry approaches to elucidate the mechanism of action of Antroquinonol. Our results suggest that Antroquinonol prevents posttranslational prenylation of the Ras and Ras-related proteins through inhibition of the enzyme isoprenyltransferase, ultimately causing cancer cell death.

2. Materials and methods

2.1. Cell lines and cell culture

Human lung cancer (A549 and H838), liver cancer (HepG2 and Hep3B), and leukemia (K562 and THP-1) cell lines were obtained from American Type Culture Collection (Rockville, MD, USA). A549 was cultured in Dulbecco's modified Eagle's medium. H838, K562 and THP-1 were cultured in RPMI-1640 medium. HepG2 and Hep3B were cultured in MEM. All cells were cultured at 37 °C in 5% CO_2 in culture media supplemented with 10% fetal bovine serum (FBS) and 100 U/mL streptomycin and penicillin. For treatment, cells were seeded in six-well plates at 6.25×10^5 cells/well. On the following day, the media was changed to serum-free media, and cells were serum-starved for 24 h. Antroquinonol [4] was dissolved in DMSO and diluted to the required concentration in serum-free medium. Cultures were then treated with diluted Antroquinonol as indicated. After treatment, cells were washed with cold phosphate-buffered saline (PBS) and lysed using RIPA buffer containing phosphatase and protease inhibitors. Cell culture media and related reagents were purchased from Invitrogen (Rockville, MD).

2.2. Immunoblot analysis

Proteins were resolved on 12.5% SDS-polyacrylamide gels. Blots were blocked with 3% bovine serum albumin (BSA) and probed with a 1:1000 dilution of antibodies LC3B (Novus Biologicals, Cambridge, UK), Ras, GAPDH, or Rho (Millipore, Temecula, CA). Secondary antibodies were conjugated to horseradish peroxidase, which was detected using a 3,3′-diaminobenzidine substrate kit (Vector Laboratories, Burlingame, CA). The immunoreactive bands were quantified by densitometry using Image-Pro Plus software (Media Cybernetics, Silver Spring, MD).

2.3. CCK-8 cell viability assay

Cell viability was measured using Cell Counting Kit-8 (CCK-8, Enzo Life Sciences, Farmingdale, NY). After treatment, CCK-8 solution was added to each well and incubated for 4 h. The concentration of formazan was measured with a spectrophotometer at an absorbance wavelength of 450 nm. Cell viability was expressed as a percentage of the corresponding control.

2.4. SDS-PAGE-based prenyltransferase assay

In vitro prenylation reactions were performed in 20 μL reaction buffer (50 mM HEPES, pH 7.2, 50 mM NaCl, 5 mM $MgCl_2$, 5 mM DTT, and 20 μM GDP) mixed with 3 μg FTase (Jena, Germany), 25 μM NBD-FPP, and 2 μg H-Ras^{GST} in the presence or absence of various concentrations of Antroquinonol. Reactions were incubated for 2 h at 37 °C and quenched by SDS-PAGE sample buffer. The mixtures were resolved by 15% SDS-PAGE. The gel was scanned using a Typhoon 9400 scanner (GE Healthcare, UK) (excitation laser, 473 nm; emission cutoff filter, 510 nm) followed by staining with Coomassie blue. The fluorescent bands were quantified using Image-Pro Plus software.

2.5. Immunofluorescent and DAPI staining

Cells were seeded onto glass coverslips. After an overnight incubation, cells were treated with Antroquinonol for 24 h. After treatment, cells were fixed with 4% paraformaldehyde and permeabilized with 0.1% Triton X-100. Cells were blocked in 3% BSA and then incubated with a LC3B antibody at room temperature. After washing, cells were incubated with a fluorescein isothiocyanate-conjugated secondary antibody (Life Technologies, Scotland, UK) at room temperature for 60 min. Cells were mounted with Dapi-Fluoromount-G™ (SouthernBiotech, Birmingham, USA) and visualized by confocal fluorescence microscopy using a Zeiss LSM 780 plus ELYRA S.1.

2.6. Molecular docking

The amino acid sequence for FTase (Accession no.: 1JCQ_A) was downloaded from the National Center for Biotechnology Information protein database. A CDOCKER–A CHARMm-based molecular docking algorithm was applied to predict and assess the interaction between Antroquinonol and the FTase CAAX box [18]. In order to limit bias, all user-adjustable parameters were kept at their default settings.

2.7. Kinetics and affinity detection by BIAcore

The kinetics and affinity of protein FTase and GGTase-I against Antroquinonol respectively were measured using BIAcore T200 (Uppsala, Sweden, GE). Recombinant FTase and GGTase-I proteins were expressed using Baculovirus expression system and purified by Ni column. Proteins FTase and GGTase-I were immobilized on the Series S Sensor Chip CM5 using a standard amine coupling method. A scouting procedure was performed to establish an appropriate concentration range of analyte and monitor association/dissociation time for affinity measurement. The experiment was performed at 25 °C. Different concentrations of Antroquinonol were finally injected to the reference, FTase and GGTase surfaces at a flow rate of 30 μL/min. In each injection, association and dissociation phases were monitored for 240 s and 120 s respectively. One buffer-only injection was included for double reference. The carry-over injections refer to buffer injections that follow the sample injections during each cycle were set as control. All

Table 1
IC_{50} values of compounds used in this study.

	A549	H838	Hep3B	HepG2	K562	THP-1
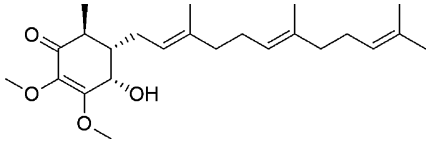 Antroquinonol	3.24 ± 0.35	2.96 ± 0.05	3.74 ± 0.35	6.42 ± 0.08	5.12 ± 0.83	2.22 ± 0.03
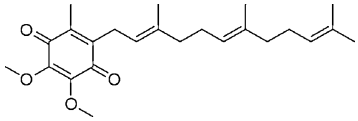 Quinone 3 (Q3)	–	22.56 ± 6.45	–	–	–	–
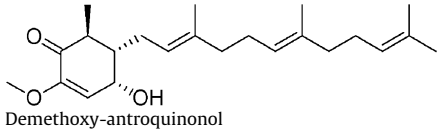 Demethoxy-antroquinonol	–	11.34 ± 4.17	–	–	–	–
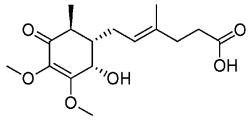 Meta2	–	> 100	–	–	–	–
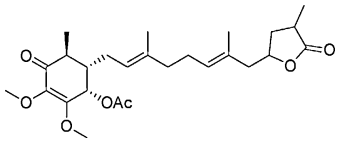 4-acetyl-antroquinonol B	–	> 100	–	–	–	–
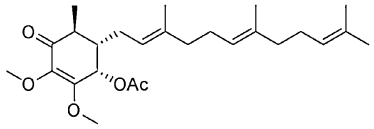 Antroquinonol-OAC	–	> 100	–	–	–	–
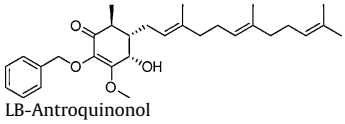 LB-Antroquinonol	22.61 ± 2.24	25.56 ± 6.54	9.06 ± 3.03	27.03 ± 6.06	–	–
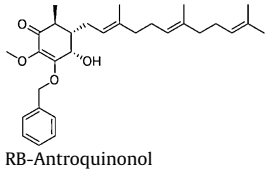 RB-Antroquinonol	6.68 ± 0.75	3.41 ± 1.43	7.46 ± 7.06	8.98 ± 0.97	–	–

IC_{50} values (μM) were determined by CCK-8 cell viability assay. Values were presented as means ± S.E.M.

concentrations of Antroquinonol were repeated. All data were analyzed by BIAcore T200 evaluation software version 1.0.

2.8. Statistical Analysis

Results were expressed as the mean ± standard error of the mean (SEM) of three independent experiments. A single factor pair-wise ANOVA statistical analysis was conducted to determine the significance in differences. A two-tailed *P*-value of less than 0.05 was considered significant.

3. Results

3.1. Determining the cytotoxic effects of Antroquinonol and its derivatives, analogues, and a metabolite

To determine whether the cytotoxic effects of Antroquinonol correlate with the presence of *Ras* mutations, cell lines derived from human lung cancer (A549 and H838), liver cancer (HepG2 and Hep3B), and leukemia (K562 and THP-1) with wild-type *Ras* (H838, Hep3B, and K562) or mutant *Ras* (A549, HepG2, and THP-1) were used. Cell viability was measured after 48 h of Antroquinonol treatment. The cell lines and their IC_{50} in increasing order were THP-1 (2.22 μM) < A549 (3.24 μM) < H838 (3.32 μM) < Hep3B (3.74 μM) < K562 (5.12 μM) < HepG2 (6.42 μM) (Table 1). Thus, sensitivity to Antroquinonol did not correlate with *Ras* gene status, as Antroquinonol exhibited excellent cytotoxic activity in all cell lines.

Next, the IC_{50} values for Antroquinonol derivatives (Antroquinonol-OAC and RB-/LB-Antroquinonol), a metabolite (meta2), and analogues isolated from filamentous *A. camphorata* (quinone Q3, demethoxy-Antroquinonol, and 4-acetyl-Antroquinonol) were determined in H838 cells. The results indicated that the ′-hydroxy group and the farnesyl group of Antroquinonol were important for its cytotoxic effects. Further, RB-Antroquinonol was even more cytotoxic than the prototype, Antroquinonol.

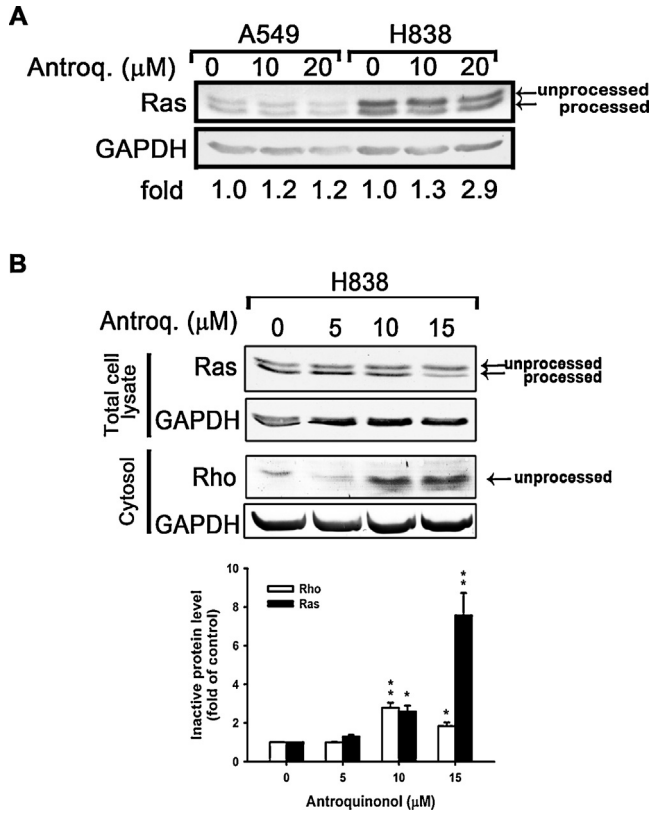

Fig. 1. Antroquinonol inhibits Ras and Rho processing in cancer cell lines. (A) A549 and H838 cells were treated with different concentrations of Antroquinonol and grown under serum-free (no FBS) conditions for 24 h. The fold of unprocessed to processed Ras was indicated below the blots. (B) H838 cells were treated with different concentrations of Antroquinonol and grown under serum-free (no FBS) conditions for 24 h. Whole cell lysates and cytoplasmic extracts were then immunoblotted with Ras or Rho antibodies as indicated respectively. A duplicate membrane was probed with a GAPDH antibody. The relative expression level of unprocessed to processed Ras or unprocessed form of Rho was quantified by densitometry and normalized with GAPDH. The experiments were conducted three times. Bars represent the mean ± SEM. $^{*}P < 0.05$; $^{**}P < 0.01$.

3.2. Antroquinonol-inhibited Ras and Rho processing in cancer cells

To better understand the cellular signaling pathways that lead to Antroquinonol-mediated cancer cell death and to more precisely identify the cytosolic target of Antroquinonol, we investigated the contribution of Ras and Rho proteins. Experiments were conducted using A549 and H838 cells, which were treated with different concentrations of Antroquinonol for 24 h. Antroquinonol caused an accumulation of unprocessed Ras in both cell lines (Fig. 1A and B). Furthermore, an abnormal accumulation of cytosolic inactive Rho protein was also detected (Fig. 1B).

3.3. Antroquinonol inhibited protein FTase activity in vitro and was competitive with FPP in cell culture

Posttranslational modification of Ras is essential for its activation. The first step committing Ras to become active is prenylation by the enzyme FTase [19,20]. Comparison of the chemical structures of Antroquinonol and FPP, which is a prenyl group donor for Ras, showed that both compounds have the same C15 lipid chain. Thus, we evaluated the effects of Antroquinonol on in vitro protein FTase activity and FPP-dependent Ras prenylation in cell culture. Results indicated that Antroquinonol alone significantly enhanced accumulation of unprocessed Ras. Further, FPP alone potentiated Ras processing in H838 cells. Competition

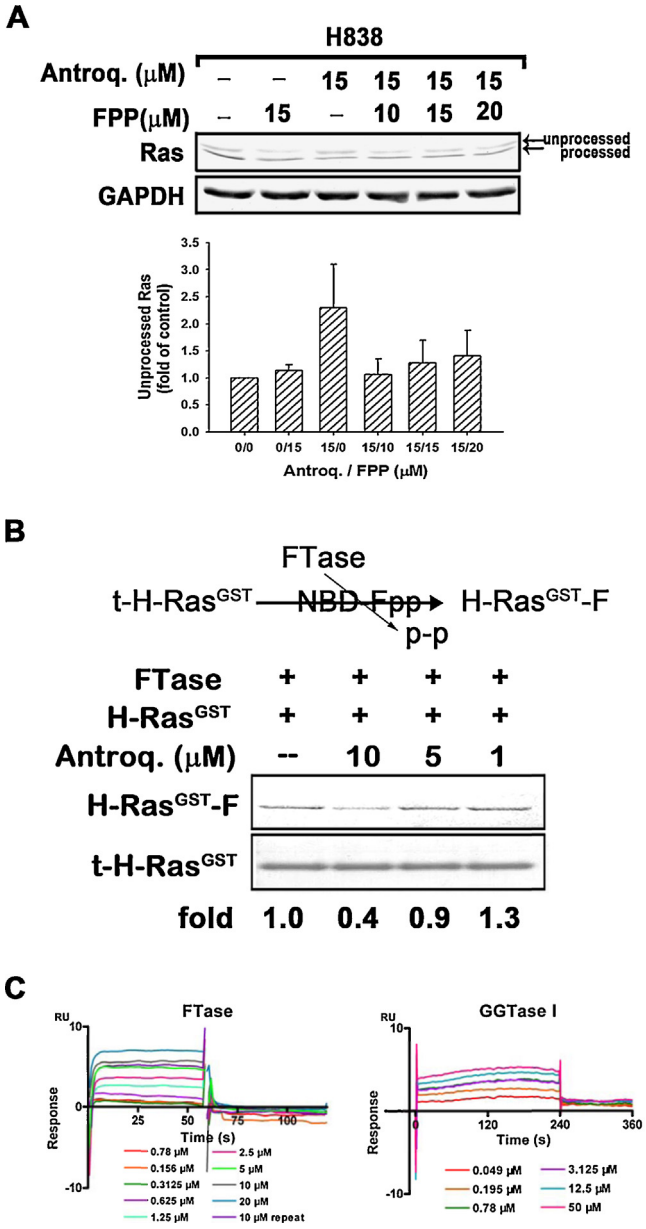

Fig. 2. Antroquinonol inhibits the prenylation activity of FTase and GGTase-I in vitro and competes with FPP within cells. (A) H838 cells stimulated with either Antroquinonol or FPP as indicated for 24 h. Whole cell lysates were then immunoblotted with a Ras antibody. A duplicate membrane was probed with a GAPDH antibody. The relative expression level of unprocessed to processed Ras was quantified by densitometry. The experiments were conducted three times. (B) SDS-PAGE of fluorescently labeled H-Ras-GST after prenylation with NBD-FPP mediated by FTase. The lower panel shows the same gel stained with Coomassie blue. The fold of unprocessed to processed Ras was indicated below the blots. (C) Direct binding of Antroquinonol to FTase and GGTase-I individually by BIAcore analysis. The binding affinity of Antroquinonol with FTase (left panel) and GGTase-I (right panel) respectively were reflected by response unit (RU) values. The kinetic measurements wwere performed using a set of serial dilutions as indicated.

assays showed that FPP neutralized the effect of Antroquinonol on Ras processing at concentrations as low as 10 μM (Fig. 2A). In addition, an in vitro enzymatic activity assay demonstrated that Antroquinonol achieved dose-dependent inhibition of FTase activity (Fig. 2B). The binding affinities between Antroquinonol and FTase and another important prenyltransferase, GGTase-I, were measured using surface Plasmon resonance (BIAcore). The KD value for FTase and GGTase-I were determined to be 2.986×10^{-6} M and 5.014×10^{-7} M respectively, suggesting that Antroquinonol

have the strongest binding capacity to GGTase-I. Taken together, our data provided evidence for the direct binding of Antroquinonol to prenyltransferase such as FTase and GGTase-I in this study.

3.4. Molecular docking of Antroquinonol on protein FTase

Using the crystal structure of FTase (PDB ID 1JCQ) as a template, we built a docking model to characterize the interaction between Antroquinonol and the CAAX motif in FTase. Docking studies showed that Antroquinonol and FPP bind in a similar orientation to the FTase active site (Fig. 3A and B). The farnesyl group of Antroquinonol lies in the hydrophobic cavity and interacts with a number of conserved aromatic residues. The ring structure with the functional groups of Antroquinonol and the diphosphate moiety of FPP are located near the α/β-subunit interface. The docking model can also be used to explain differences in the cytotoxic profiles of Antroquinonol analogues. It has been shown that the number of isoprene units influences the binding affinity of isoprenoids for FTase [21]. The ′-hydroxy group of Antroquinonol may form intermolecular hydrogen bonds with the tyrosine residue, Y300b (Fig. 3C). In addition, the spatial arrangement of the ring structure of Antroquinonol indicated that the 3-methoxy group is located in an unoccupied space near the interface of the FTase subunits. Thus, it was likely that demethoxy-Antroquinonol would show an IC_{50} only slightly less than the prototype, Antroquinonol. These results provide important structural insights into the specific architecture of Antroquinonol and the CAAX motif in FTase, which will help with the rational design of active Antroquinonol analogues (Fig. 3D).

3.5. Antroquinonol enhanced autophagic activity in cancer cells

Our previous investigations indicated that Antroquinonol induces apoptosis and/or autophagic cell death in human cancer cell lines via the PI3K/mTOR pathway [3]. Ras lies upstream of PI3K and has been demonstrated to negatively regulate autophagic activity in RasVal12-transformed NIH3T3 cells [22]. Here, the level of Antroquinonol-induced autophagic conversion of LC3B-1 to LC3B-II in a lung cancer cell line was measured by immunoblot analysis of LC3B. Further, LC3B-II-associated autophagosomes were observed by confocal microscopy (Fig. 4).

4. Discussion

Antroquinonol exhibits various anticancer, antioxidant, anti-inflammatory, and autoimmune activities. However, the actual mechanism of action of Antroquinonol remains unknown. In this study, we investigated the possible mechanism of action of Antroquinonol in cancer cell lines. We provide evidence that:

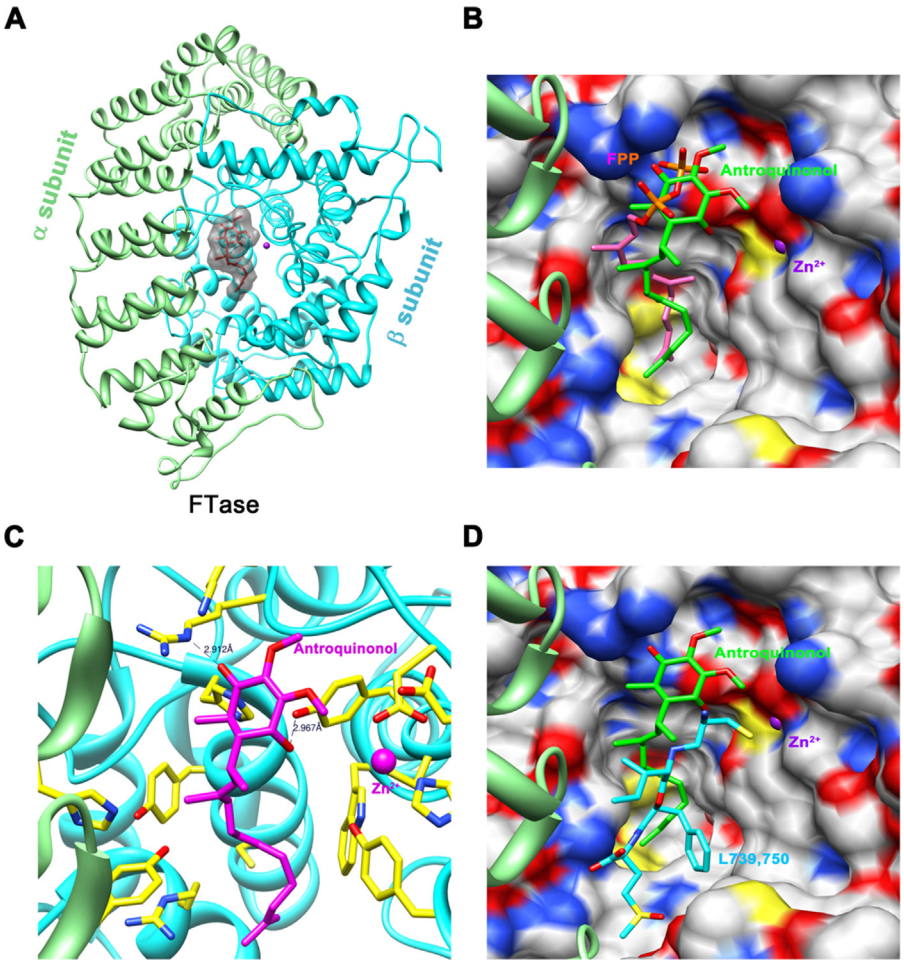

Fig. 3. The model structure of human FTase in complex with Antroquinonol, CIFM-derived L739,750 peptidomimetic, and FPP substrate. (A) Ribbon cartoons of FTase complexed with Antroquinonol. (B) Simultaneous binding of Antroquinonol (green) and FPP (purple) to FTase. (C) Ribbon cartoons of FTase complexed with Antroquinonol. Putative hydrogen bonds are represented by dashed lines. (D) Ribbon cartoons of FTase complexed with Antroquinonol and CIFM-derived L739,750.

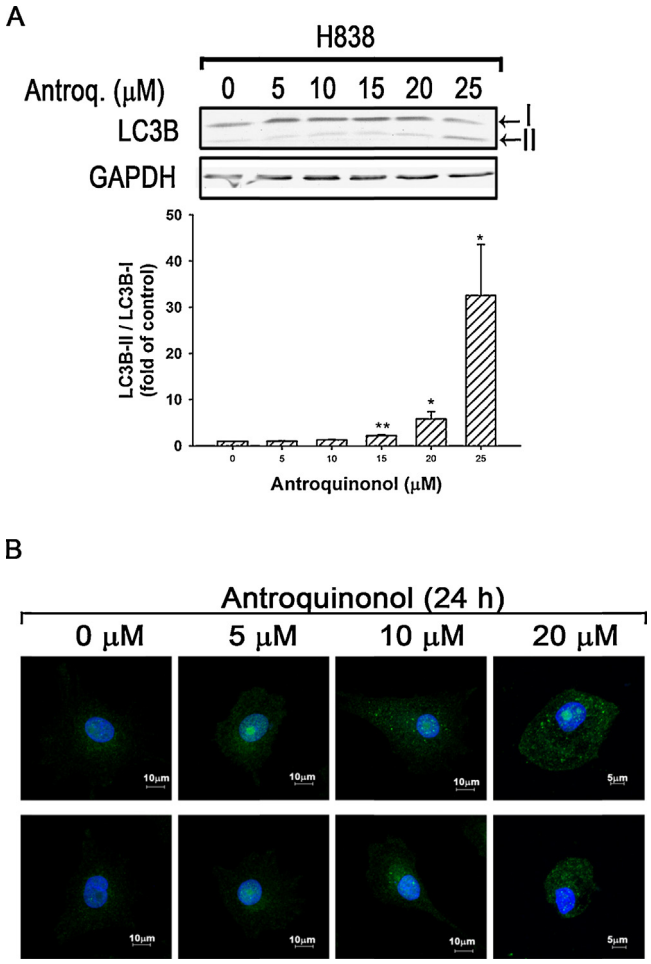

Fig. 4. Antroquinonol induces autophagic activity in H838 cells. H838 cells were treated with different concentrations of Antroquinonol and grown under serum-free conditions. (A) Cells were harvested at 0, 24 and 48 h following treatments and subjected to immunoblotted with Beclin-1 antibody. (B) Whole-cell lysates were prepared at 24 h following treatments and subjected to immunoblotted with an LC3B antibody. A duplicate membrane was probed with a GAPDH antibody. The relative expression level of LC3B-I to LC3B-II was quantified by densitometry. (C) The distribution of endogenous LC3B in autophagosomes was detected by confocal microscopy. The experiments were conducted three times. Bars represent the mean ± SEM. $^{*}P < 0.05$, $^{**}P < 0.01$.

- Antroquinonol inhibited isoprenyltransferase activity in vitro;
- posttranslational processing of Ras and Rho was inhibited by Antroquinonol in a dose-dependent manner;
- increased LC3B-II was coordinated with an increase in autophagosome formation after Antroquinonol treatment of cancer cells

Thus, we propose that Antroquinonol interferes with prenylation of Ras and Rho proteins through inhibition of isoprenyltransferase, such as FTase or GGTase-I, in cancer cells.

Ras proteins are small GTPases that appear to be engaged in multiple signaling pathways, leading to complex and divergent effects[23]. Prenylation is essential for the normal function and transforming activity of the Ras superfamily proteins. Thus, agents that block Ras prenylation have been developed to interfere with cancer cell survival and proliferation [24]. Antroquinonol is a novel farnesylated quinone derivative isolated from *A. camphorata*. Docking studies showed that the farnesyl isoprenoid tail of Antroquinonol inserts into the central cavity of the FTase β-subunit similar to the farnesyl group of FPP. Here, enzymatic assays revealed that Antroquinonol inhibited FTase in a dose-dependent manner in vitro. The inactive form of Ras increased in cancer cells after Antroquinonol administration. Furthermore, the results of the BIAcore analysis also indicated that Antroquinonol binds with different affinity to FTase and GGTase-I. Taken together, our data provided evidence for the direct binding of Antroquinonol to FTase and GGTase-I. It was inferred that Antroquinonol interacts with isoprenyltransferase to prevent Ras-related proteins processing inside cancer cells.

Interestingly, we have found the moderate positive correlation between IC_{50} value of Antroquinonol in cancer cell lines and Ras, Rho and epidermal growth factor receptor (EGFR) expression (Fig. 5). The data suggested that the protein level of Ras, Rho and EGFR, rather than the presence of mutations in the *Ras* and *EGFR* genes, is the major determinant of Antroquinonol-induced cytotoxicity in cancer cells.

Our previous studies revealed that Antroquinonol triggers antitumor activity through the inhibition of PI3K-Akt-mTOR pathway [6,7]. Here, we provide evidence that Antroquinonol indirectly inhibits Ras and Rho processing through inhibition of isoprenyltransferase activity. It has been observed that cooperation between Ras and Rho families of small GTPases are required for PI3K activation [25], which in accordance with our findings. Thus, the possible signaling pathways that contribute to Antroquinonol-mediated antitumor activity are summarized in Fig. 6. The Ras/Rho-PI3K-Akt-mTOR pathway, which is associated with proliferation, motility, metabolism, and differentiation, is

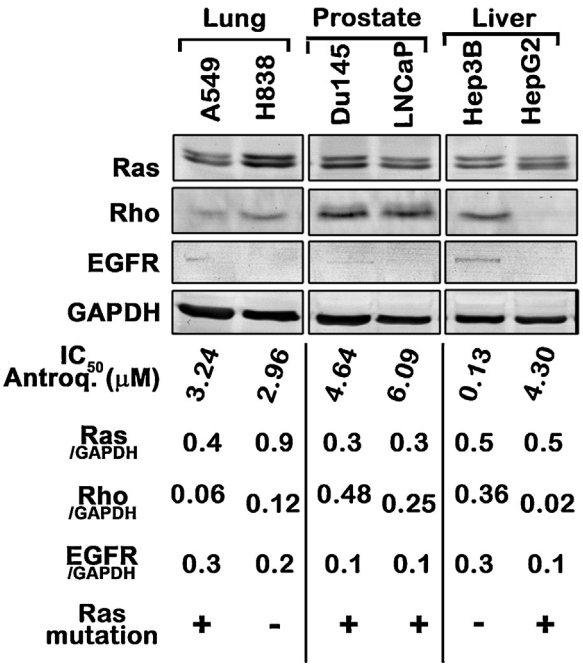

Fig. 5. The cytotoxic activity of Antroquinonol was correlated with protein levels of Ras, Rho and EGFR in cancer cell lines. Whole cell lysates were resolved by SDS-PAGE and amounts of Ras, Rho, EGFR or GAPDH were detected by immunoblot analysis. The relative expression level of proteins were quantified by densitometry and normalized with GAPDH. The experiments were conducted three times.

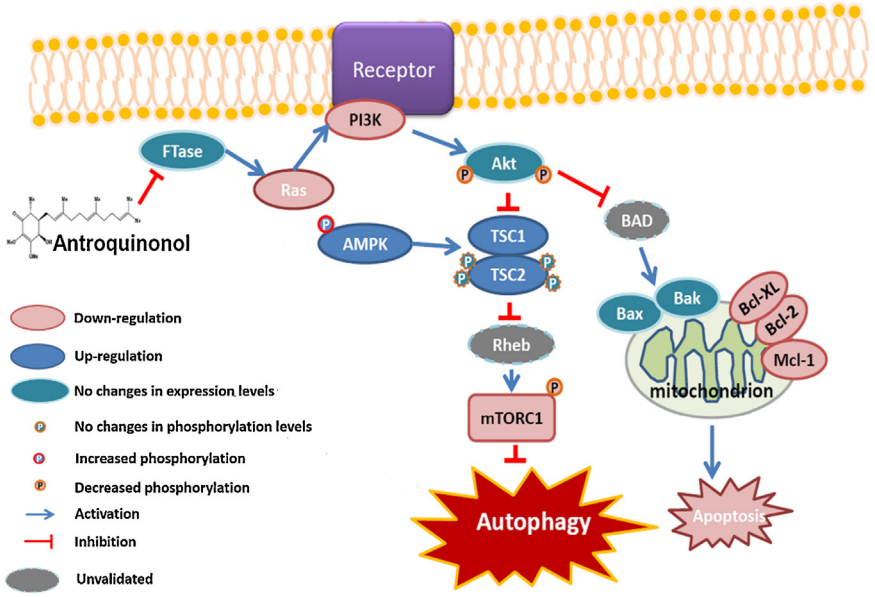

Fig. 6. Schematic diagram illustrating the proposed mechanism of action of Antroquinonol. Lines with end arrows indicate activation, whereas those with perpendicular bars at the end indicate inhibition. A red color indicates down-regulation and blue color indicates up-regulation. A gray color with a dotted circle indicates molecules that have not been validated. "P" indicates phosphorylation.

inhibited in response to Antroquinonol. We believed that multiple signaling pathways are simultaneously involved in response to Antroquinonol stimulation. Thus, Antroquinonol may promote its anticancer effects by regulating cross talk in a complex signaling network that results in apoptosis and autophagy.

In summary, this is the first report to elucidate a potential mechanism for the anticancer activity of Antroquinonol. Inhibition of isoprenyltransferase activity suppresses prenylation of multiple signaling molecules, interfering with downstream signaling. Ras is a pivotal signaling protein in a complex network that regulates several aspects of normal cell growth and malignant transformation. Activating mutations in Ras, especially K-Ras, frequently occur in human cancers. Thus, targeting Ras is a promising strategy for treating cancer. Based on the biochemical characterization and molecular docking analysis in this study, Antroquinonol inhibits Ras and Rho processing via inhibition of the enzyme isoprenyltransferase activity, such as FTase and GGTase-I, ultimately resulting in cell death. Antroquinonol is a new molecular entity isolated from *A. camphorata*. The natural origin of Antroquinonol is now undergoing Phase 2 clinical evaluation in patients with non-small cell lung cancer. Understanding the mechanism of action of Antroquinonol will facilitate the identification of predictive biomarkers and will aid in the rational design of future clinical trials.

Disclosure of interest

The authors declare that they have no conflicts of interest concerning this article.

Acknowledgement

We thank Ms. Shu-Chen Shen (Scientific Instrument Center of Academia Sinica, Taiwan) for her excellent technical assistance with confocal microscopy.

References

[1] Harvey AL. Natural products in drug discovery. Drug Discov Today 2008;13:894–901.
[2] Wu SH, Ryvarden L, Chang TT. Antrodia camphorata (“niu-chang-chih”), new combination of a medicinal fungus in Taiwan. Bot Bull Acad Sinica 1997;38:273–5.
[3] Kumar VB, Yuan T-C, Liou J-W, Yang C-J, Sung P-J, Weng C-F. Antroquinonol inhibits NSCLC proliferation by altering PI3K/mTOR proteins and miRNA expression profiles. Mutat Res 2011;707:42–52.
[4] Tsai P-Y, Ka S-M, Chao T-K, Chang J-M, Lin S-H, Li C-Y, et al. Antroquinonol reduces oxidative stress by enhancing the Nrf2 signaling pathway and inhibits inflammation and sclerosis in focal segmental glomerulosclerosis mice. Free Radic Biol Med 2011;50:1503–16.
[5] Kumar KJS, Chu F-H, Hsieh H-W, Liao J-W, Li W-H, Lin JC-C, et al. Antroquinonol from ethanolic extract of mycelium of Antrodia cinnamomea protects hepatic cells from ethanol-induced oxidative stress through Nrf-2 activation. J Ethnopharmacol 2011;136:168–77.
[6] Chiang P-C, Lin S-C, Pan S-L, Kuo C-H, Tsai IL, Kuo M-T, et al. Antroquinonol displays anticancer potential against human hepatocellular carcinoma cells: a crucial role of AMPK and mTOR pathways. Biochem Pharmacol 2010;79:162–71.
[7] Yu C-C, Chiang P-C, Lu P-H, Kuo M-T, Wen W-C, Chen P, et al. Antroquinonol, a natural ubiquinone derivative, induces a cross talk between apoptosis, autophagy and senescence in human pancreatic carcinoma cells. J Nutr Biochem 2012;23:900–7.
[8] Shimizu N, Ohtsubo M, Minoshima S. MutationView/KMcancerDB: a database for cancer gene mutations. Cancer Sci 2007;98:259–67.
[9] Casey PJ, Solski PA, Der CJ, Buss JE. p21ras is modified by a farnesyl isoprenoid. Proc Natl Acad Sci U S A 1989;86:8323–7.
[10] Maurer-Stroh S, Eisenhaber F. Refinement and prediction of protein prenylation motifs. Genome Biol 2005;6(6):R55 [Epub 2005 May 27].
[11] Crul M, de Klerk GJ, Beijnen JH, Schellens JH. Ras biochemistry and farnesyl transferase inhibitors: a literature survey. Anticancer Drugs 2001;12:163–84.
[12] Sebti SM, Hamilton AD. Anticancer activity of farnesyltransferase and geranylgeranyltransferase-I inhibitors: prospects for drug development. Exp Opin Investig Drugs 1997;6:1711–4.
[13] Cox AD, Der CJ. Farnesyltransferase inhibitors and cancer treatment: targeting simply Ras? Biochim Biophys Acta 1997;1333:F51–71 [Reviews on Cancer].
[14] Gibbs JB, Oliff A. The potential of farnesyltransferase inhibitors as cancer chemotherapeutics. Annu Rev Pharmacol Toxicol 1997;37:143–66.
[15] Fiordalisi JJ, Johnson RL, Weinbaum CA, Sakabe K, Chen Z, Casey PJ, et al. High affinity for farnesyltransferase and alternative prenylation contribute individually to K-Ras4B resistance to farnesyltransferase inhibitors. J Biol Chem 2003;278:41718–27.
[16] Whyte DB, Kirschmeier P, Hockenberry TN, Nunez-Oliva I, James L, Catino JJ, et al. K- and N-Ras are geranylgeranylated in cells treated with farnesyl protein transferase inhibitors. J Biol Chem 1997;272:14459–64.
[17] Lebowitz PF, Prendergast GC. Non-Ras targets of farnesyltransferase inhibitors: focus on Rho. Oncogene 1998;17(11 Reviews):1439–45.
[18] Wu G, Robertson DH, Brooks CL, Vieth M. Detailed analysis of grid-based molecular docking: a case study of CDOCKER – A CHARMm-based MD docking algorithm. J Comput Chem 2003;24:1549–62.
[19] Reiss Y, Goldstein JL, Seabra MC, Casey PJ, Brown MS. Inhibition of purified p21ras farnesyl:protein transferase by Cys-AAX tetrapeptides. Cell 1990;62(1):81–8.
[20] Kato K, Cox AD, Hisaka MM, Graham SM, Buss JE, Der CJ. Isoprenoid addition to Ras protein is the critical modification for its membrane association and transforming activity. Proc Natl Acad Sci U S A 1992;89:6403–7.
[21] Lane KT, Beese LS. Thematic review series: lipid posttranslational modifications. Structural biology of protein farnesyltransferase and geranylgeranyltransferase type I. J Lipid Res 2006;47:681–99.
[22] Furuta S, Hidaka E, Ogata A, Yokota S, Kamata T. Ras is involved in the negative control of autophagy through the class I PI3-kinase. Oncogene 2004;23:3898–904.
[23] Buday L, Downward J. Many faces of Ras activation. Biochimi Biophys Acta 2008;1786:178–87.
[24] Appels NMGM, Beijnen JH, Schellens JHM. Development of Farnesyl transferase inhibitors: a review. Oncologist 2005;10:565–78.
[25] Yang HW, Shin MG, Lee S, Kim JR, Park WS, Cho KH, et al. Cooperative activation of PI3K by Ras and Rho family small GTPases. Mol Cell 2012;47(2):281–90. http://dx.doi.org/10.1016/j.mol.cel.2012.05.007 [Epub 2012 Jun 7].